 doi:10.20944/preprints202207.0299.v1

Article

Comparative Analysis of Battery Thermal Management System using Biodiesel Fuels

Mansour Al Qubeissi [1 *], Ayob Mahmoud [1], Moustafa Al-Damook [2], Zinedine Khatir [3], Hakan Serhad. Soyhan [4,5] and Raja Mazuir Raja Ahsan Shah [1,4]

[1] Faculty of Engineering, Environment and Computing, Coventry University, Coventry CV1 2JH, United Kingdom
[2] Renewable Energy Research Center, University of Anbar, Iraq
[3] School of Engineering and the Built Environment, Faculty of Computing, Engineering and the Built Environment, Birmingham City University, Birmingham B4 7XG, United Kingdom
[4] Department of Mechanical Engineering, Sakarya University, Esentepe Campus, Sakarya, 54050, Turkiye
[5] Team-San Co., Teknokent, Esentepe Campus, Sakarya, 54050, Turkiye
*Corresponding author: ac1028@coventry.ac.u

Abstract: This paper focuses on the comparative analysis of lithium-ion batteries (LIB) thermal management with aim to maintain working temperature in the range 15 ℃ – 35 ℃. This is to prevent thermal runaway and high temperature gradients. The proposed approach is to employ the biodiesel, situated inside the diesel/LIB powered hybrid electric vehicle, to supply as fuel and coolant. A 3S2P LIB module is simulated using Ansys-Fluent CFD software tool. The system without a coolant shows that LIB has exceeded the optimum maximum temperature, which leads to shortened life-cycle and poor performance. Four fatty acid methyl ester biodiesels are used as coolants, namely palm, karanja, jatropha, and mahua oils. When compared with conventional methods of cooling, using air and 3M Novec liquid, the palm biodiesel coolant proves to be the best option to maintain LIB temperature within the optimum working range. With the use of palm biodiesel, the system is estimated to lightweight the BTMS by 43%, compared to the case when 3M Novec is used to maintain the same temperature range.

Keywords: battery thermal management; biodiesel fuel; hybrid vehicle; Li-ion battery; cooling technology

1. Introduction

The world is moving towards a series of energy security, environmental and economic challenges, with the fossil fuel slow depletion and high pollutions [1–3]. As such, the term 'renewable energy' is more popular than ever. The current renewable energy resources for alternative liquid fuels are biofuels [4]. In Diesel engines, biodiesel is the renewable alternative. Biodiesel has so far been only used in conjunction with direct combustion engines (e.g., [5–7]), but it has not been facilitated for the cooling of lithium-ion batteries (LIB) in hybrid electric vehicles (HEV). On the other hands, LIB have been used in battery electric vehicles (BEV) and HEV applications as a source of energy due to the recent world shift to clean technologies and the aligned policies to meet the net zero emission. The high temperature values and contrasts can have significant effects on the LIB performance, capacity, life-cycle and safety [8,9]. As LIB discharges and charges its power, heat is generated, gradually increasing its temperature [10]. While excessive heat is generated in hot counties such as in Gulf Region leading to weak marketing of HEV. An effective battery thermal management system (BTMS) can be implemented to maintain the optimal operating temperature of LIB within the recommended range of 15℃ – 35℃ [11,12]. This range is found essential for extending the LIB service life, reducing maintenance costs, and increasing safety[13,14]. In addition, BTMS needs to achieve uniform temperature across LIB to avoid faster cell degradation and for good voltage balancing at

Preprints (www.preprints.org) | NOT PEER-REVIEWED | Posted: 20 July 2022 doi:10.20944/preprints202207.0299.v1

temperature [14]. For larger LIB pack, which consists of several LIB modules (small packs), it is difficult to control the temperature homogeneity due to the LIB cell arrangement.

BTMS uses several thermal management techniques such as air cooling, liquid cooling and Phase Change Materials (PCM) [15]. Liquid cooling is deemed the most efficient due to higher liquid coolant thermal conductivity compared to air and PCM [16]. However, the high density of liquid coolant increases the vehicle weight, and subsequently consumes more energy from LIB. With the emergence of BEV and HEV, the importance of efficient thermal management systems for LIB packs have increased. In [17], the finding outlines the main thermal issues that occurs when temperatures exceed this range which includes thermal runaway, affecting the safety of the vehicle and reducing the overall lifespan of LIB cells. Thermal runaway can cause the electrolyte structure of LIB cells to break down thus increasing the temperature to an uncontrollable point which negatively affects the vehicle safety [18]. In addition to reducing the maximum temperature, the temperature gradient across the LIB module and pack must not exceed 5 ℃ as it would cause LIB cells to degrade faster due to uneven voltage discharges [14]. An experiment devised by [19] compared two LIB packs, one with even temperature distribution and one with an uneven temperature distribution. The study concluded that the LIB pack with uneven temperature distribution degraded 7% faster. Over time, this uneven temperature distribution would cause the LIB to significantly lose its potential charge. Many techniques are developed and used to reduce the max temperature of LIB, including air and liquid coolings [20,21].

It has been known that the best form of BTMS is liquid based with direct cooling [11]. The present work is made to envisage a conjugate heat transfer system that can utilise the temperature of HEV LIBpack within the optimum range of 15 °C– 35 °C [11,12]. The system is based on direct cooling methods using biodiesel as a coolant, which in turn reduces the weight of the vehicle and ultimately eliminates the need for additional coolant. The design will be analysed using the commercial Computational Fluid Dynamics (CFD) software tool of ANSYS-Fluent® and verified where possible. Also, the vehicle lightweighting is a crucial design aspect for increasing lifecycle and reducing fuel consumption; hence, adding economic and emission reduction benefits [22]. Also, waste heat recovery is a promising solution to clean and efficient HEV [23]. The current research in BTMS will be assessed with special attention to direct liquid and air-based systems. The thermal airflow systems embedding liquid (3M Novec coolant) and air-based methodologies will then be reviewed including a selection of four biodiesels. It is hypothesised that using a biodiesel will be a viable option in BTMS with extra benefits in vehicle lightweighting [24]. Four dielectric biodiesel fuels are used in our comparative analysis, namely palm, jatropha, mahua, and karanja Fatty Acid Methyl Esters (FAME).

As one can see from the literature, BTMS has a vital role in the power system lifecycle, performance, and cost aspects. There has been extensive research in this field. However, most of previous studies have focussed on the classical approach of cooling the LIB or showing the importance of providing accurate predictions. There has been only one concept on the use of fuel as coolant to reduce the dependence on heavy liquids [24]. To the best of our knowledge, there has not been a single study on the use of biofuels as LIB coolants. Hence, the work presented in this paper is first of its kind. In what follows we show the method used for the numerical analysis and verification of data in Section 2. The results of BTMS using various approaches are presented in Section 3. The research findings are summarised in Section 4.

2. The model and system specifications

In the following section details of the methods used in the analysis including conjugate heat transfer physics and CFD setup are laid out. The section will also look at the four different biodiesels selected to be used as coolants whilst also including properties of

Preprints (www.preprints.org) | NOT PEER-REVIEWED | Posted: 20 July 2022 doi:10.20944/preprints202207.0299.v1

conventional methods in air and 3M Novec. A mesh convergence analysis is performed to ensure the mesh does not affect the results thus increasing the accuracy.

2.1. LIB module description

The study is focussed on a 30 Ah LIB module that consists of several prismatic LIB cells arranged in series and parallel connection. A series connection increases the LIB module total voltage whereas a parallel connection increases the capacity of the LIB module meaning a slower discharge rate. The LIB cells are configured as 3 cells in series and 2 in parallel creating a 3S2P LIB module, as depicted in Figure 1. Following [25], the simulation of LIB module was assumed sufficient to replace the periodic flow behaviour in a full LIB pack system considering the highest temperature predictions.

LIB cells were attached using tabs and busbars to form the complete LIB module. The distance between LIB cells were set to 5 mm giving room for a fluid enclosure to allow for conjugate heat transfer and thus the cooling of LIB cells. LIB cell specifications were important in this analysis to ensure for a true representation of a HEV LIB pack. The LIB component materials and parameters are listed in Tables 1 and 2 respectively.

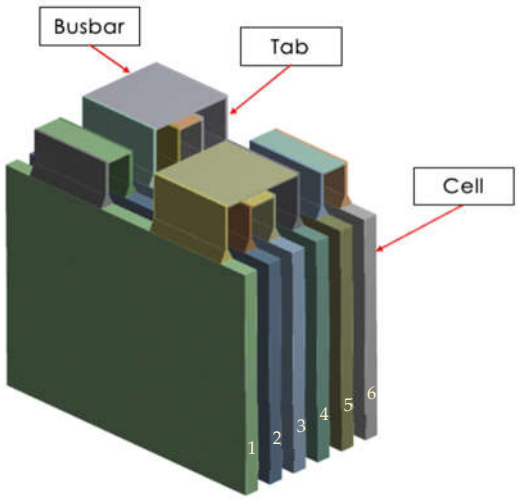

Figure 1. Schematic of the 3S2P LIB module.

Table 1. LIB module component material properties.

Properties	Aluminium (Busbar)	Copper (Tab)	LIB cell material
Density (kg/m^3)	2719	8978	2029
Specific heat (J/kg·K)	871	381	678
Thermal conductivity (W/m·K)	202.4	387.6	18.2
Electrical conductivity	3.541 x 10^7	5.8 x 10^7	5.8 x 10^7

Table 2. Specifications of LIB cell used in this study.

Nominal capacity (A·h)	30
C-rate	3
Maximum voltage (V)	4.2
Minimum voltage (V)	2.7
Height (mm)	100
Width (mm)	100
Thickness (mm)	5

Preprints (www.preprints.org) | NOT PEER-REVIEWED | Posted: 20 July 2022 doi:10.20944/preprints202207.0299.v1

An enclosure was adopted in Ansys fluent where the fluid will flow around LIB cells. This enclosure consists of a rectangular inlet and outlet with section breaks that guide the fluid in an alternating pattern around each LIB cell. This would ensure the fluid is contacting every LIB cell surface without it being very large thus decreasing the mass of the system. Figure 2 shows the enclosure geometry. The main function of the enclosure is to reduce the LIB cell maximum temperature and to create an even temperature difference across the LIB module. This will improve the LIB performance and efficiency.

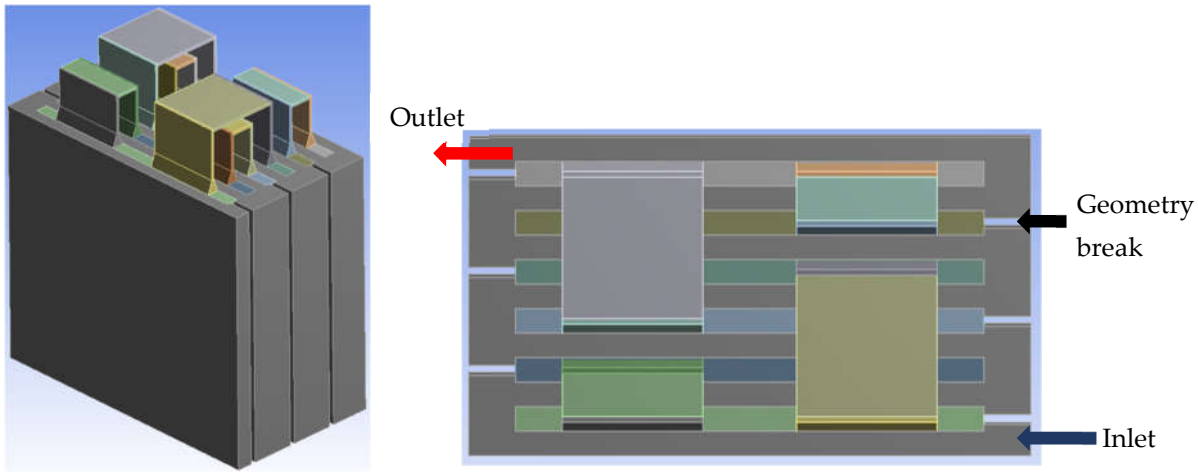

Figure 2. Schematic of the enclosure geometry, showing (a) isometric view and (b) topview of the domains.

2.2. Basic heat transfer equations

Conjugate heat transfer occurs when there is direct contact between a fluid and solid. This is also called forced convection. To calculate the convective heat transfer of a system, the following formula is used [26]:

$$\dot{Q}_{Convection} = hA(T_s - T_\infty) \quad (1)$$

where h is the convective heat transfer coefficient, A is the surface area, T_s is surface temperature and T_∞ is the free stream temperature of the fluid. As the fluid passes the cells, a thermal boundary layer is generated. The Reynolds number of the fluid affects the thickness of this boundary layer which is calculated with the following formula [26]:

$$Re = \frac{\rho V L}{\mu} \quad (2)$$

where ρ is the fluid density, V is the fluid velocity, L is the characteristic length and μ is the dynamic viscosity of the fluid. These values are all known, therefore making it simple to calculate the Reynolds number of the fluid. The formula suggests that an increase in velocity would increase the Reynolds number thus increasing the boundary layer thickness. The Prandtl number is another non-dimensional parameter that defines the relative thickness of the thermal boundary layer. It is obtained using the relationship [26]:

$$Pr = \frac{\mu C_p}{k} \quad (3)$$

where μ is the dynamic viscosity of the fluid, C_p the specific heat and k the conductive heat transfer coefficient. The Nusselt Number is the final dimensionless parameter which is used to determine the convective heat transfer coefficient. Nusselt Number denotes the convective heat transfer through the fluid layer, relative to the conduction of the fluid. Nusselt Number is defined as follows [26]:

Preprints (www.preprints.org) | NOT PEER-REVIEWED | Posted: 20 July 2022 doi:10.20944/preprints202207.0299.v1

$$\mathrm{Nu} = \frac{hL_c}{k} \tag{4}$$

where L_c is the characteristic length and k is the conductive heat transfer coefficient. If the Nusselt number increases, it means the convection of the fluid is more effective. For laminar and turbulent flows, the following formula are used to calculate *Nu* using Reynolds and Prandtl numbers as [26]:

$$\text{Laminar} \rightarrow \mathrm{Nu} = \frac{hL}{k} = 0.664\ \mathrm{Re}_L^{1/2}\mathrm{Pr}^{1/3} \tag{5}$$

$$\text{Turbulent} \rightarrow \mathrm{Nu} = \frac{hL}{k} = 0.037\ \mathrm{Re}_L^{4/5}\mathrm{Pr}^{1/3} \tag{6}$$

2.3. Mesh Independence test

In order to solve this complex problem and geometry, the LIB module was meshed within Ansys-Fluent® tool. A mesh convergence analysis is performed. The number of elements used in the mesh was reduced from a highly refined mesh to coarser ones until the mesh did not affect the solution stability and convergence was achieved. As such, the optimised mesh helped for accurate results and computational time efficiency. To ensure the mesh convergence was correct, the temperature values and gradients across the LIB module were monitored for the solution consistency. The mesh convergence study was applied to the air cooling system, with the results illustrated in Figure 3 to show the effects of the number of mesh elements on the domain temperature.

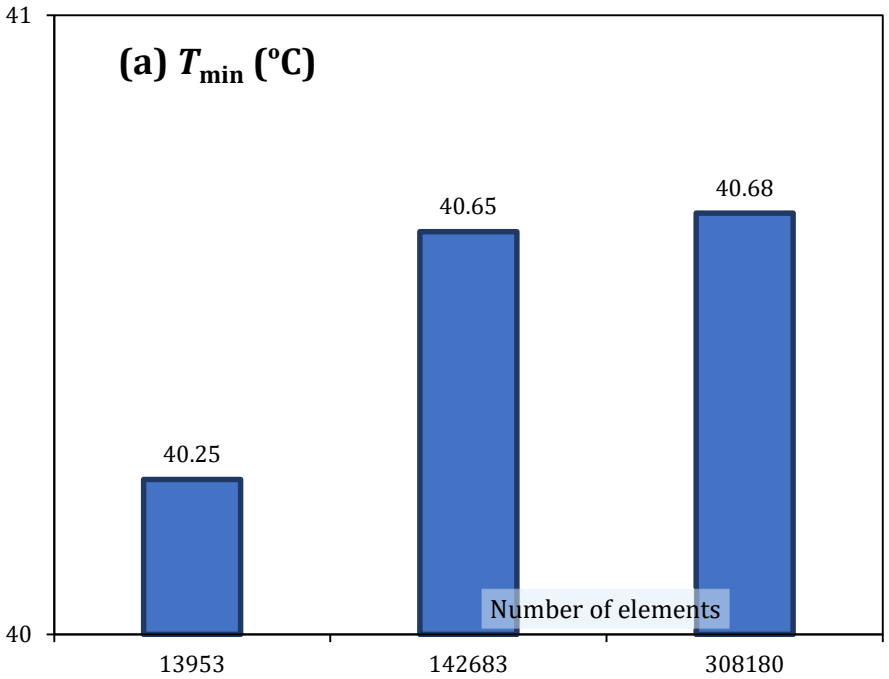

Preprints (www.preprints.org) | NOT PEER-REVIEWED | Posted: 20 July 2022 doi:10.20944/preprints202207.0299.v1

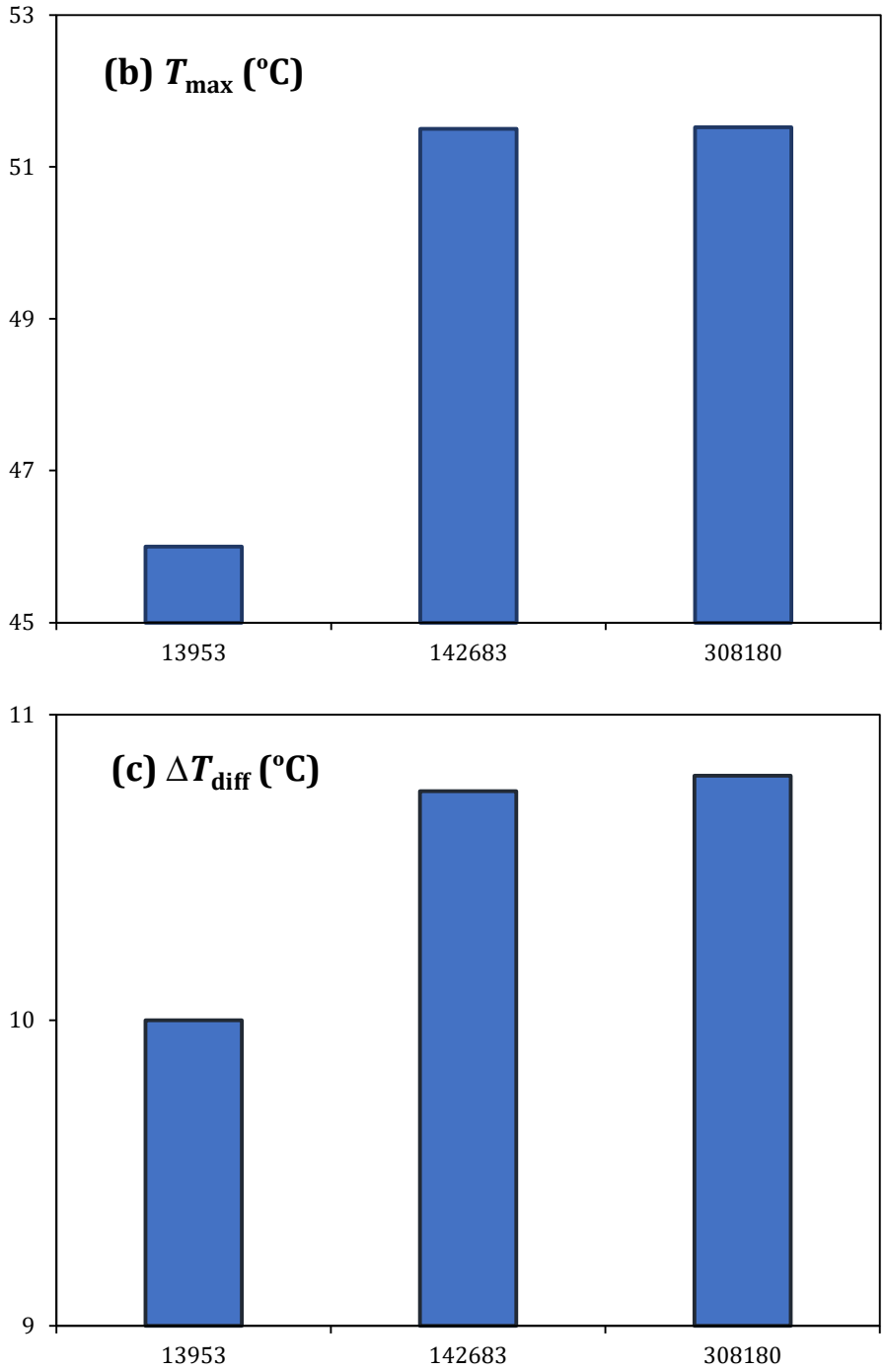

Figure 3. Temperatures across the domains versus number of mesh elements, showing (a) maximum temperature, (b) minimum temperature, and (c) maximum temperature difference.

A hexahedral meshing type is used for the convenience of mapping our rectangular fluid and solid domains. Hexahedral elements are economic; i.e. tend to be more efficient for the same number of nodes compared to the tetrahedral and polyhedral ones [27]. This convergence study clearly demonstrated the effects of the mesh on the results. As the number of elements were increased, the results consistency reveal sufficient mesh independence check in Figure 3. Any further attempt to decrease mesh size would mean more unnecessary computational power was needed increasing the run time of each simulation. Between a mesh size of 2 and 1.5mm, there was a negligible difference in the three results. Consequently, a mesh size of 2mm was chosen which has high accuracy based on the results. The final meshed model is depicted in Figure 4. This mesh consists of hexahedral

Preprints (www.preprints.org) | NOT PEER-REVIEWED | Posted: 20 July 2022 doi:10.20944/preprints202207.0299.v1

elements with an element size of 2mm with a total of 142683 elements that make up the complete BTMS ready for the simulations.

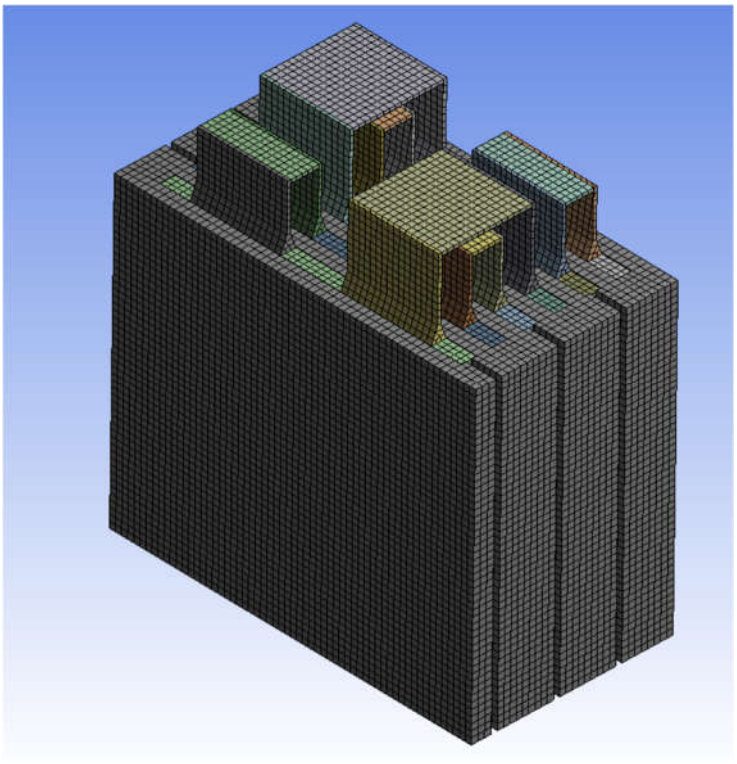

Figure 4. Final mesh of LIB with enclosure which consists of 142683 hexahedral elements.

2.4. Biodiesel and conventional coolants

Four biodiesels were analysed and compared to each other to select the best cooling performance in BTMS. . , Two conventional coolants, air and 3M Novec 7100 werealso simulated in conjunction with the biodiesel cooling. This approach has createda good comparison and allowed the effectiveness of the biodiesel to be assessed alongside current cooling methods. Four dielectric FAME biodiesels were investigated for BTMS, namely: palm, jatropha, mahua, and karanja. Their thermodynamic and transport properties are inferred from [28,29].

Biodiesels are a form of alternative fuels that are made from natural substances such as oils, animal fats and plants [30]. These fuels are more economically friendly when compared with fossil fuels making it a better alternative in HEV where the aim is lowering exhaust gas emissions [30]. Palm oil biodiesel is a type of fuel made from a vegetable oil collected from palm trees. The fuel is created using methanol as a catalyst [30]. The fuel can be used directly in engines or can be mixed with diesel to produce different blends as outlined by [30]. The density of the fluid is around 865 kg/m^3 making it considerably less dense than conventional coolants such as 3M Novec (1510 kg/m^3). This would reduce overall vehicle weight and make it a more appealing option if the cooling efficiency is on par with the conventional coolants. Jatropha is a type of plant which produces seeds with an oil content of around 37% [31]. This oil is used to produce biodiesel as an alternative to fossil fuels. Mahua biodiesel is also an option as outlined [31], which is made from oil extracted from a Mahua seed. The final biodiesel in this study is Karanja. Karanja is a tree that is mostly found in India. Karanja oil can be extracted from this tree and used as a biofuel [31]. In [32], the effects of different blends of these four biodiesel fuels on their thermodynamic properties were investigated experimentally. The experiments extracted properties of the fluid at 300 K with a composition of C18:1. They showed that palm oil biodiesel wasthe least dense out of the four tested ones and has the highest heat capacity. It wasassumed that the properties wereconstant at 300 K.

Preprints (www.preprints.org) | NOT PEER-REVIEWED | Posted: 20 July 2022 doi:10.20944/preprints202207.0299.v1

Air can be used to cool LIB at a cold ambient temperature via forced convection where the fluid comes in direct contact with the LIB cells [20]. Air does not require indirect cooling making it the easiest form of cooling as well as being the cheapest and best option for ease of maintenance. However, due to the low heat capacity of air, the system is very inefficient as specified by [33]. Some studies, such as [34], have developed methods of increasing efficiency by adding fins or by optimising the compressor velocity to ensure maximum cooling is achieved. As such, an increase in the compressor power is demanded to generate higher air velocities which is not ideal in a HEV. Therefore, air cooling is considered the least effective approach due to its low density and specific heat. To increase the cooling efficiency of air, a high velocity is required meaning higher power consumption from a compressor. These issues with weight and power consumptions are reduced with the use of biodiesels fulfilling the aim of this project. .

3M Novec is used in many cooling applications such as processor cooling in computers. In recent years, 3M Novec has been employed into BTMS. BTMS employs direct cooling method due to the dielectric nature of 3M Novec making it smaller in volume when compared to an indirect cooling approach. On the other hand, the disadvantage to using 3M Novec is the high density as presented in Table 3. A sufficient amount of 3M Novec needs to be circulated through the system which requires storage of dense fluid. This storage would increase the mass of the vehicle whilst also taking valuable space.

Table 3. Cooling fluid key properties.

Coolant	Density (kg/m^3)	Viscosity (kg/ms)	Thermal Conductivity (W/mK)	Specific Heat (J/kg·K)
Palm	865	3.91 x 10^{-3}	0.172	1687.248
Jatropha	870	4.49 x 10^{-3}	0.166	1344.881
Mahua	875	4.88 x 10^{-3}	0.170	1379.166
Karanja	895	5.62 x 10^{-3}	0.172	1257.633
3M Novec 7100	1510	6.0 x 10^{-4}	0.069	1183
Air	1.225	1.79 x 10^{-5}	0.0242	1006.43

3. Results

LIB module was simulated at different discharge rates without any form of cooling and used as benchmark data. The benchmark cooling was compared with air cooling, 3M Novec cooling and biodiesels cooling to analyse their thermal performance. Finally, a brief parametric study was performed to investigate the relationship between biodiesel cooling performance and inlet velocity.

In the CFD analysis, the turbulent flow was taking into account with thermal boundary layers. *K-epsilon* turbulence model was used to accurately represent the turbulent nature of the flow whilst reducing computational time. Energy equations were enabled to allow for heat transfer in the system. It was assumed that radiation acting on the system wasnegligible. Furthermore, the following assumptions were made within the CFD workflow:

- Transient conditions – A transient setup was utilised due to the transient nature of the LIB chemical reaction,
- Velocity at the inlet was assumed to be uniform,
- Negligible radiation,
- Incompressible flow and
- Viscous flow.

As air is the least effective at lower velocities, the inlet air velocity was tested in an extended range of 0.5–3 m/s to improve the convective heat transfer as will be outlined in Section 3. For liquid (3M Novec and biodiesel fuels) cooling, the velocity was set to the range 0.09–0.5 m/s, and initial temperature to 300K.

 doi:10.20944/preprints202207.0299.v1

3.1. LIB without cooling

The LIB module was simulated at four discharge rates of 0.5C, 1C, and 3C. The temperature distribution of the LIB module is shown in Figure 5. It can be seen that the temperature homogeneity across the LIB module was affected by increasing the discharge rate. At 0.5C, LIB cell 1 and cell 4 produced the lowest temperature with a temperature difference of 0.007 °C between LIB cells. However, at 1C and 3C, the temperature difference between LIB cells was increased to 1.222 °C.

Figure 6 shows that as the discharge rate increased, the LIB module temperature rise rate was also increased in almost linear behaviour. LIB module required 11,900 seconds to reach a maximum temperature of 41 °C at 0.5C. At 1C, the LIB module required 7000 seconds to reach the maximum temperature of 57 °C. This temperature was 42% higher than the LIB maximum operating temperature of 35 °C [cite]. 3C produced higher LIB module maximum temperatures and faster rates, 105 °C (>162 % of the LIB maximum operating temperature) at 1500 seconds

Based on the LIB module temperature distribution, maximum temperature, and the temperature rise rate, it is imperative to implement effective BTMS solutions, particularly when operating at a high discharge rate. Therefore, for the remainder of this work, the simulations of other cooling methods were focused on a discharge rate of 3C.

Preprints (www.preprints.org) | NOT PEER-REVIEWED | Posted: 20 July 2022 doi:10.20944/preprints202207.0299.v1

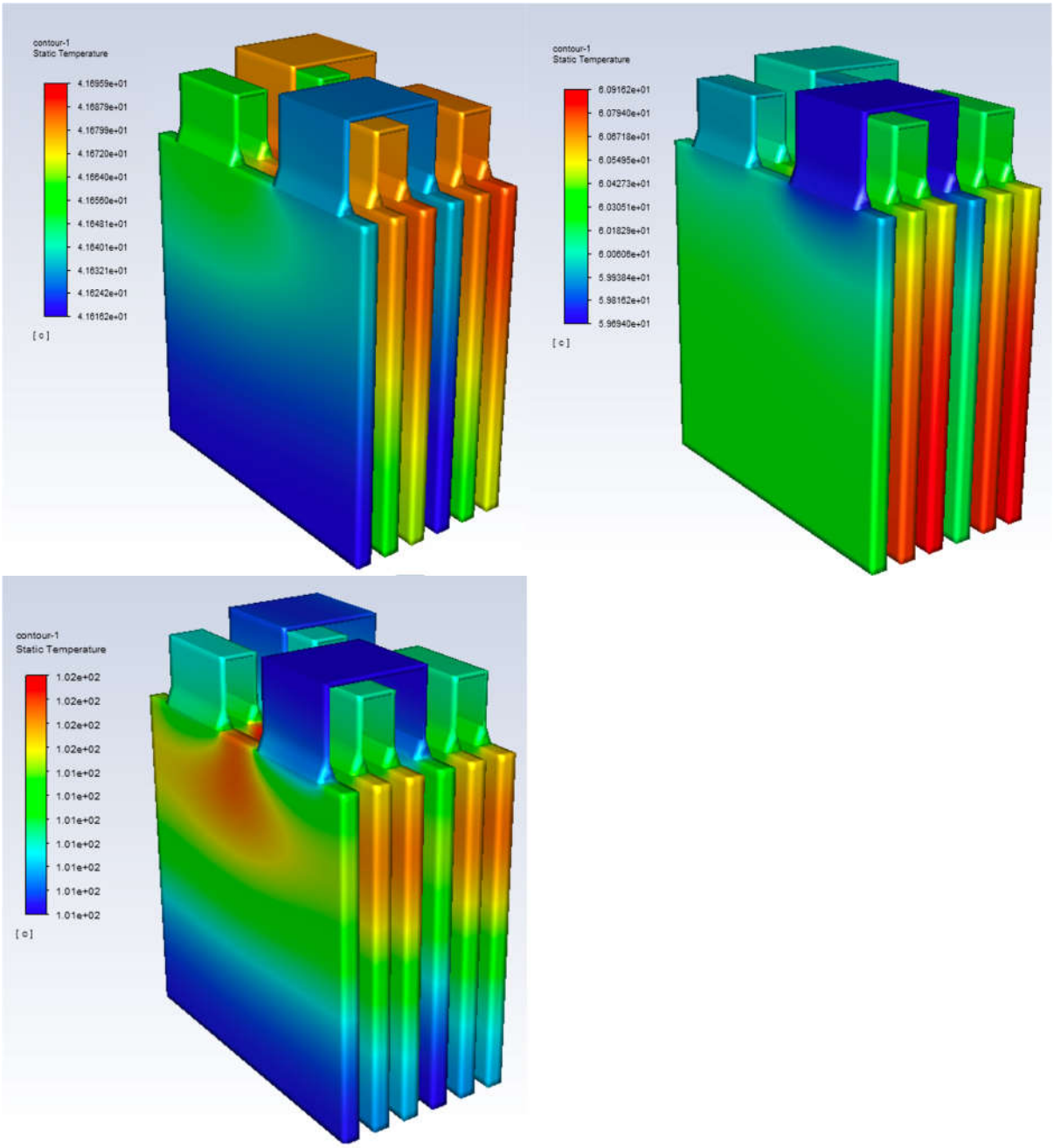

Figure 5. LIB module temperature distribution without cooling at discharge rate of a) 0.5C, b) 1C, and c) 3C.

Preprints (www.preprints.org) | NOT PEER-REVIEWED | Posted: 20 July 2022 doi:10.20944/preprints202207.0299.v1

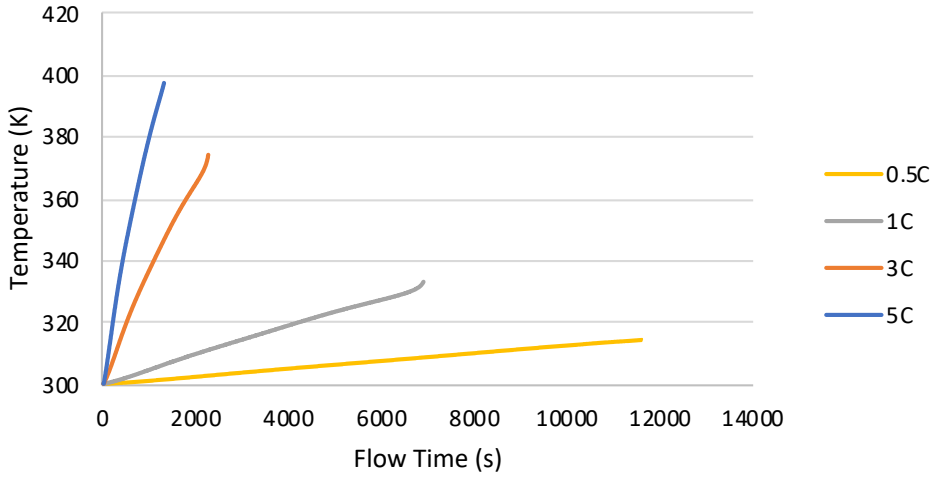

Figure 6. LIB module temperature during full depletion at different discharge rates (Convert unit to Celcius or Kelvin for consistency. Delete 5C).

3.2. Air cooling

Air cooling is the least efficient when compared to other cooling methods. Figure 7 shows the LIB module temperature distribution using air cooling at a discharge rate of 3C and inlet velocity of 3 m/s. Air cooling has significantly reduced the LIB module maximum temperature by 50% compared to no cooling temperature. However, the air cooling at 3 m/s inlet velocity was not effective to maintain the LIB module temperature below the LIB maximum operating temperature. This was due to the low density and specific heat of air which reduced the convective heat transfer [cite].

In terms of LIB temperature homogeneity, the results showed a 10 °C difference between LIB cells, which can significantly reduce the LIB voltage balancing capability and promote faster cell degradation. The air temperature towards the outlet has a large increased temperature which suggested that air was not as efficient at removing heat from the LIB module and thus needed a higher velocity. This explanation was further backed up by the LIB cell thermal behaviour as a function of discharge time in Figure 8.

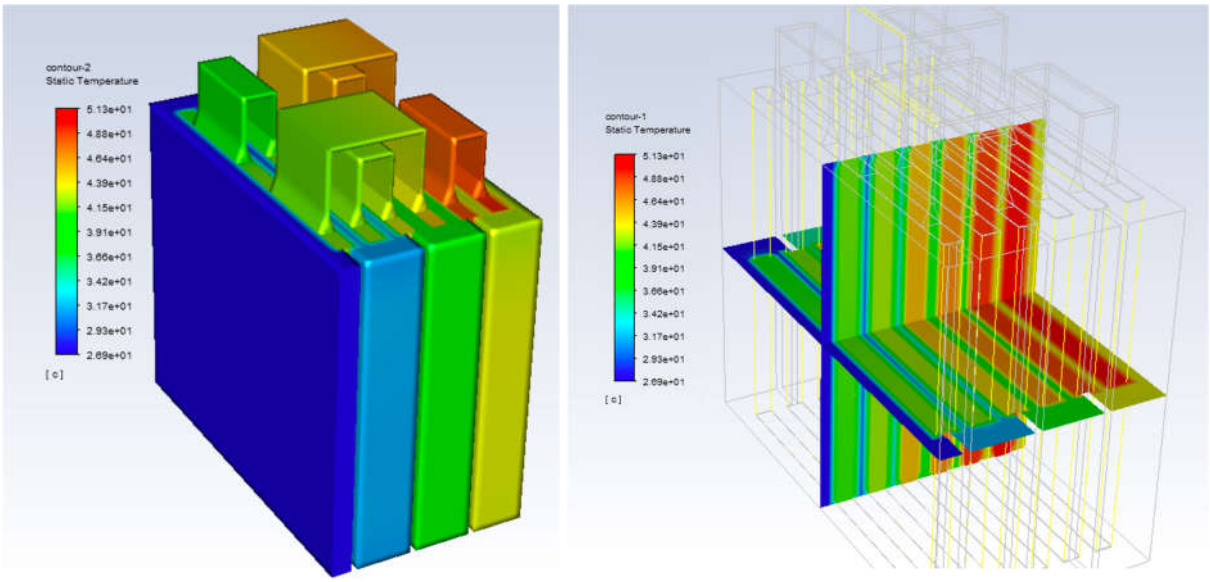

Figure 7. LIB module temperature characteristics at 3C discharge rates with air cooling a) temperature distribution , b) cell cross-section temperature.

Preprints (www.preprints.org) | NOT PEER-REVIEWED | Posted: 20 July 2022 doi:10.20944/preprints202207.0299.v1

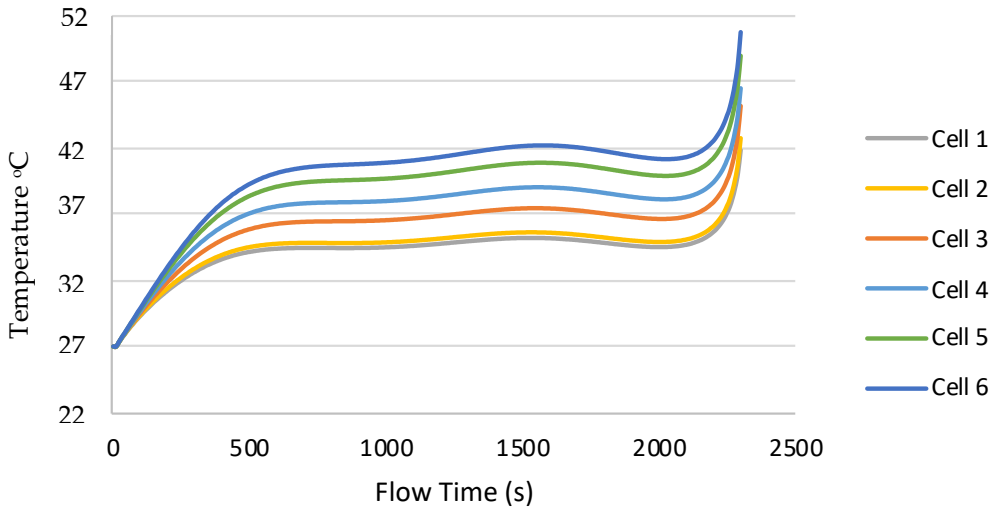

Figure 8. LIB cells temperature characteristic at 3C discharge rate with air cooling.

Air cooling caused a large temperature difference between LIB cell 1 and cell 6. However, air cooling managed to keep all LIB cell temperatures in stable conditions for most of the discharge time. Also, the air cooling kept LIB cell 1 – 4 temperatures below the maximum operating temperature. After 2200 seconds, all LIB cell temperatures started to increase due to higher internal resistance at a low state-of-charge (SOC), where LIB cell 6 temperature has the highest value of 51.3 °C. These thermal behaviours indicated that air cooling can be used as a cheaper alternative in applications where LIB does not require full discharge and hence does not reach beyond the maximum operating temperature. The high-temperature difference between LIB cells will require improvement in the air cooling by adding fins and hot plates.

3.3. 3M Novec 7100 Cooling

The temperature distribution of the LIB module based on 3M Novec cooling is shown in Figure 9. 3M Novec cooling managed to reduce the LIB module maximum temperature to 30.6 °C which was 70 % lower than the benchmark maximum temperature. The temperature difference in each LIB cell was also kept below 2 °C (See Fig. 9). The LIB module maximum temperature reduction in 3M Novec cooling suggested that it can provide a better solution compared to air cooling at a reduced working fluid velocity. However, the high specific density of 3M Novec fluid (1.4 – 1.8 kg/m^3 [35]) increases the overall vehicle weight, demands a higher pumping power, and adds up the requirement for a closed-loop storage tank.

Preprints (www.preprints.org) | NOT PEER-REVIEWED | Posted: 20 July 2022 doi:10.20944/preprints202207.0299.v1

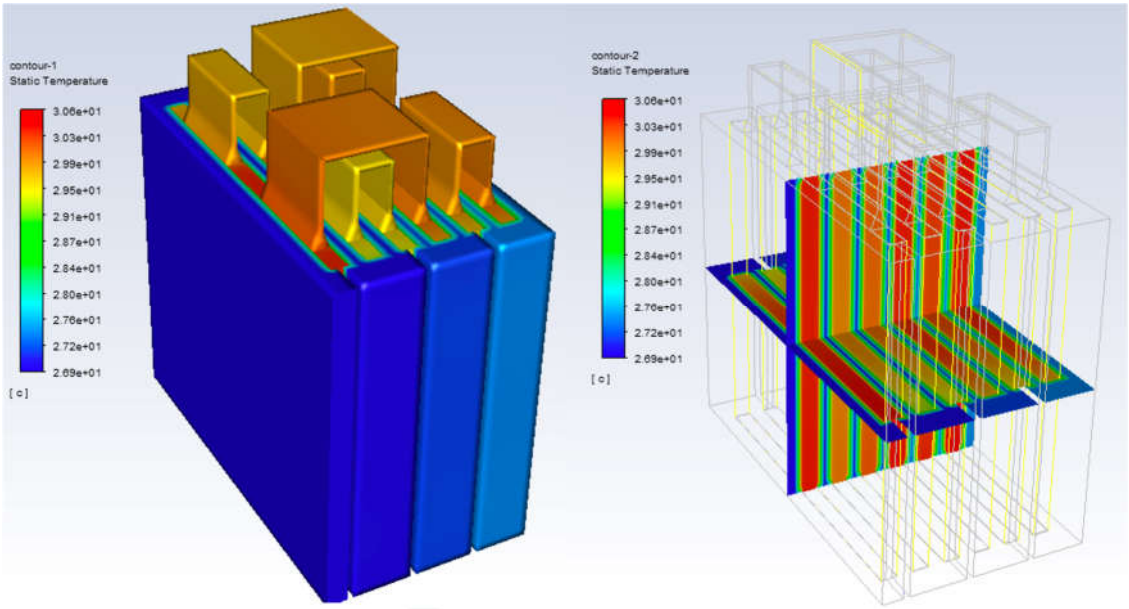

Figure 9. LIB module temperature characteristics at 3C discharge rates with 3M Novec cooling a) temperature distribution , b) cell cross-section temperature.

The temperature behaviour at full depletion of each LIB cell is shown in Figure 10. 3M Novec cooling was able to maintain the temperature of all LIB cells below 28 °C for 2000 seconds. Also, 3M Novec cooling was able to characterise the LIB cells' temperature in a fast response. Therefore, the pump can control 3M Novec fluid constantly and require less pumping energy. After 2000 seconds, it started to increase sharply to a maximum temperature of 30.35 °C due to the high LIB cell internal resistance at a lower SOC. Based on the LIB thermal behaviour using 3M Novec cooling, it is possible to let the LIB cell temperature rise in free convection environment until it reaches a certain temperature limit. Subsequently, a control system can start to pump 3M Novec fluid through the cooling system to keep the LIB cell temperature below the maximum operating temperature.

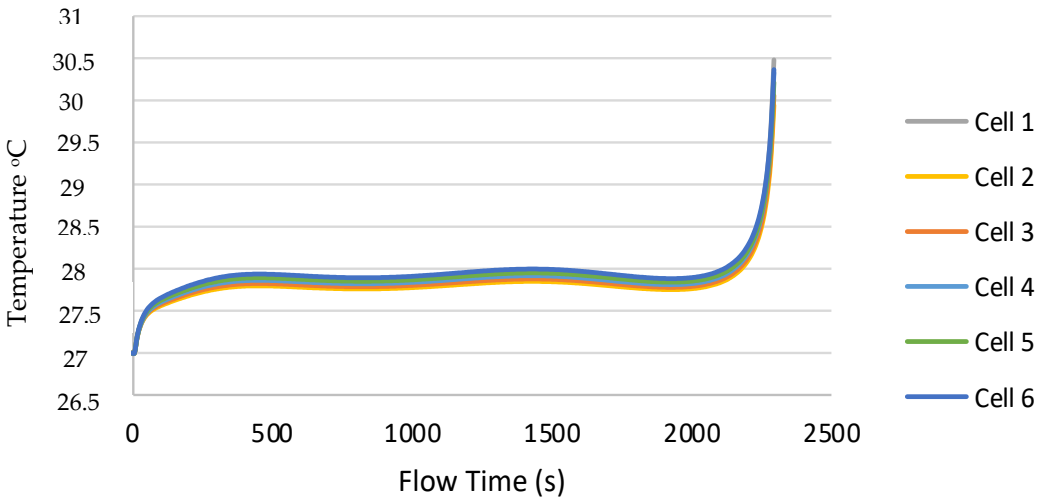

Figure 10. LIB cells temperature characteristic at 3C discharge rate with 3M Novec cooling.

3.4. Biodiesel Cooling

This section is investigating a new cooling method when using biodiesel as a coolant. From the temperature distribution in Figure 11, it is clear that the use of biodiesel as a coolant was effective in BTMS with the maximum temperature of all the simulations being

Preprints (www.preprints.org) | NOT PEER-REVIEWED | Posted: 20 July 2022 doi:10.20944/preprints202207.0299.v1

below 35°C after the LIB was fully discharged. As discussed in the literature, this LIB module's temperature characteristics can help to improve their performance efficiency and minimise cell capacity degradation. Palm oil was the marginal effective cooling medium based on having the lowest maximum temperature (<2.6%) compared to the other three biodiesels.

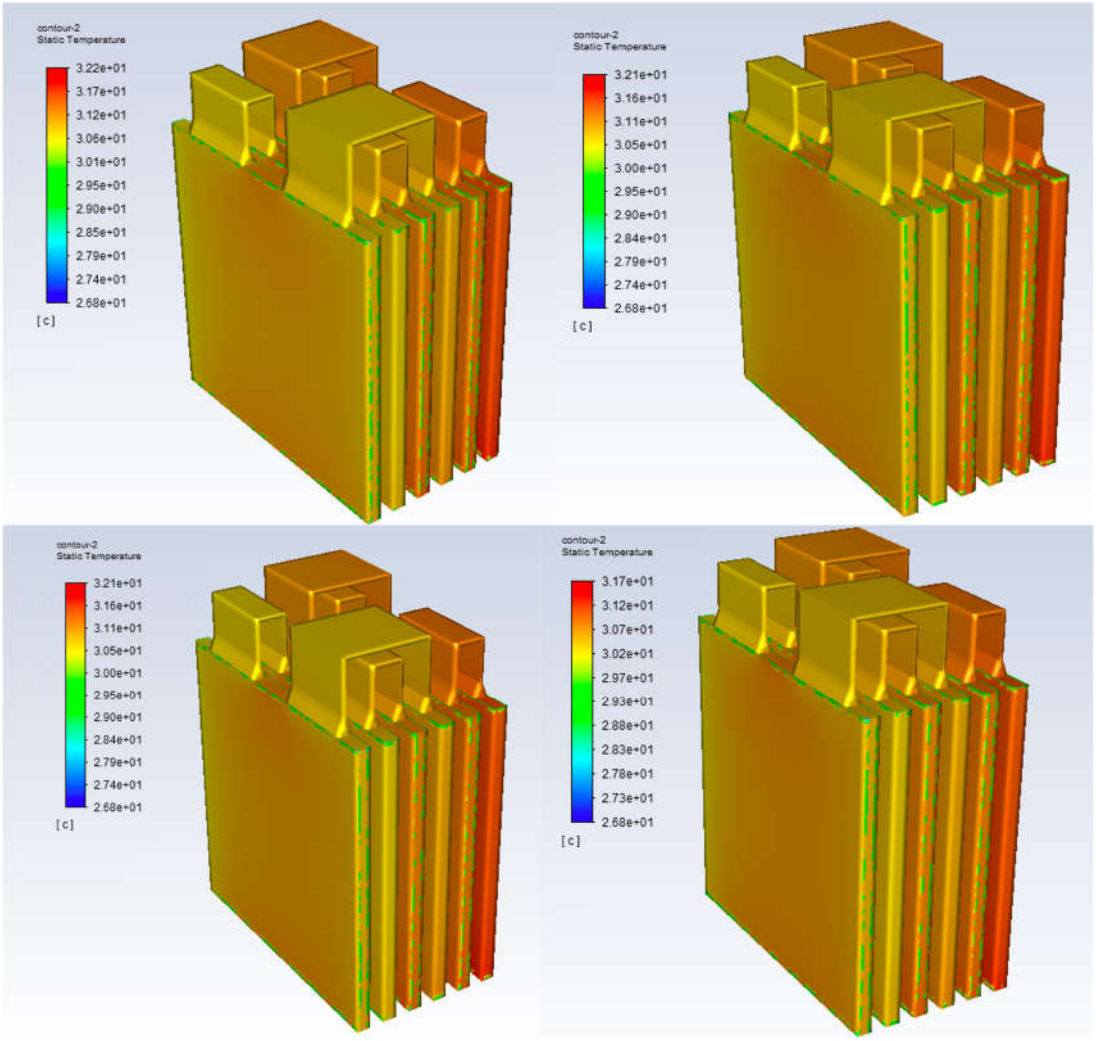

Figure 11. LIB module temperature distribution at 3C discharge rates with biodiesels cooling.

Figure 12shows the cross-section temperature of LIB cells. It can be observed that all biodiesels produced similar temperature differences of 1 °C. LIB cell 6 has the highest temperature due to the flow direction of the coolant that carried the heat from previous LIB cells. This issue can be improved by having another inlet that runs the coolant in the opposite direction such that all the cells get the maximum heat transfer. However, a double inlet system would require extra pumping power and is not necessary for this particular LIB cell configuration. A larger LIB module with more cells would require a revision in enclosure geometry or an increase in velocity based on these results.

Preprints (www.preprints.org) | NOT PEER-REVIEWED | Posted: 20 July 2022 doi:10.20944/preprints202207.0299.v1

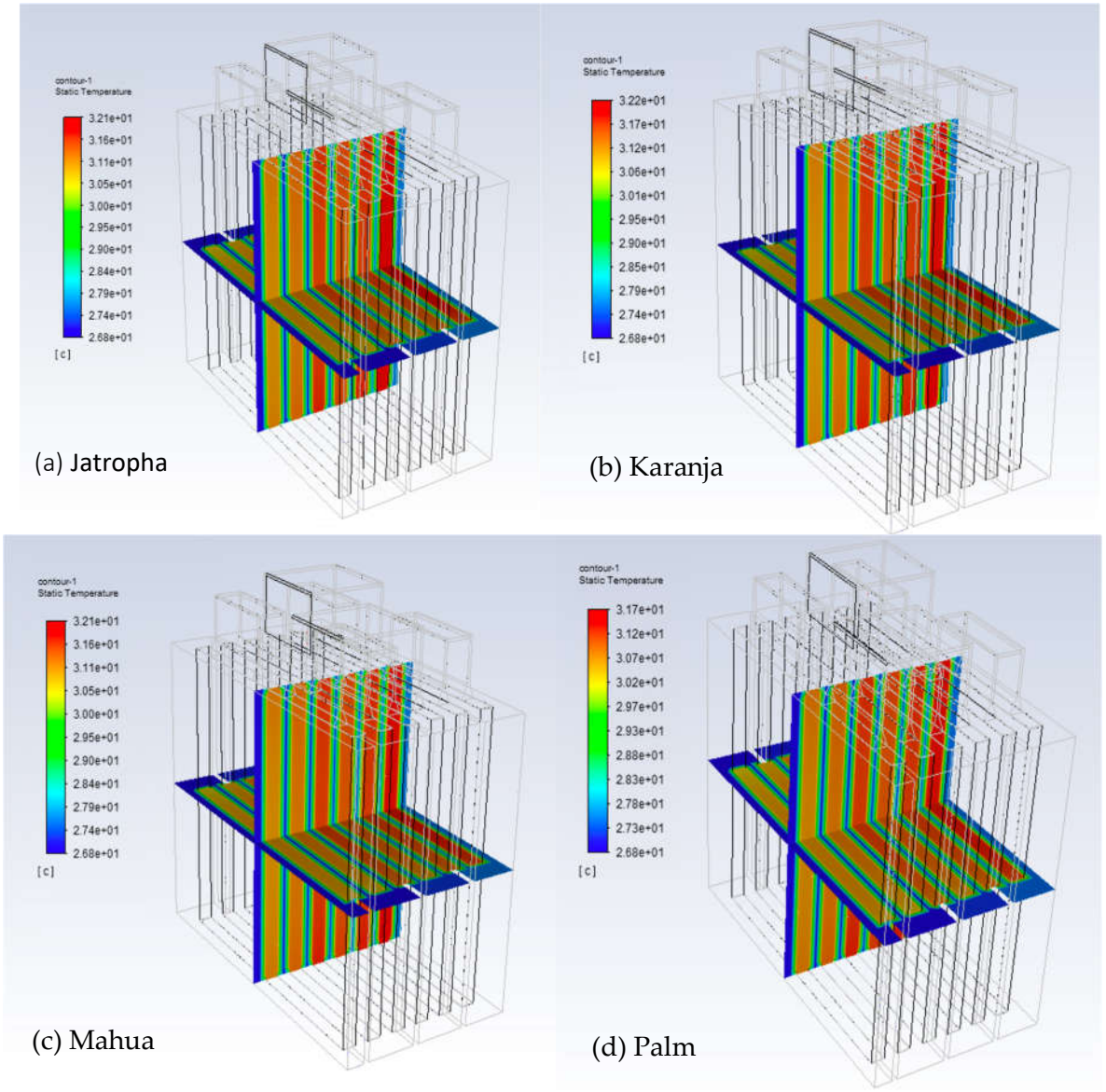

Figure 12. LIB cell cross-section temperature at 3C discharge rates with biodiesel cooling a) Jatropha, b) Karanj, c) Mahua, and d) Palm.

Figure 13 depicts the LIB cell temperature characteristics for each biodiesel cooling. The results showed a similar trend to 3M Novec cooling where biodiesel cooling were able to prevent the temperature from rising above 28 °C for 2000 seconds. The results further supported the claim that Palm is the best out of the four in managing the LIB module temperature as it has the lowest peak temperature. With Palm also being the least dense coolant, it would decrease the overall vehicle weight and extra space is formed. This is because the biodiesel is already stored in the vehicle meaning a separate storage tank is not required for another coolant.

Preprints (www.preprints.org) | NOT PEER-REVIEWED | Posted: 20 July 2022 doi:10.20944/preprints202207.0299.v1

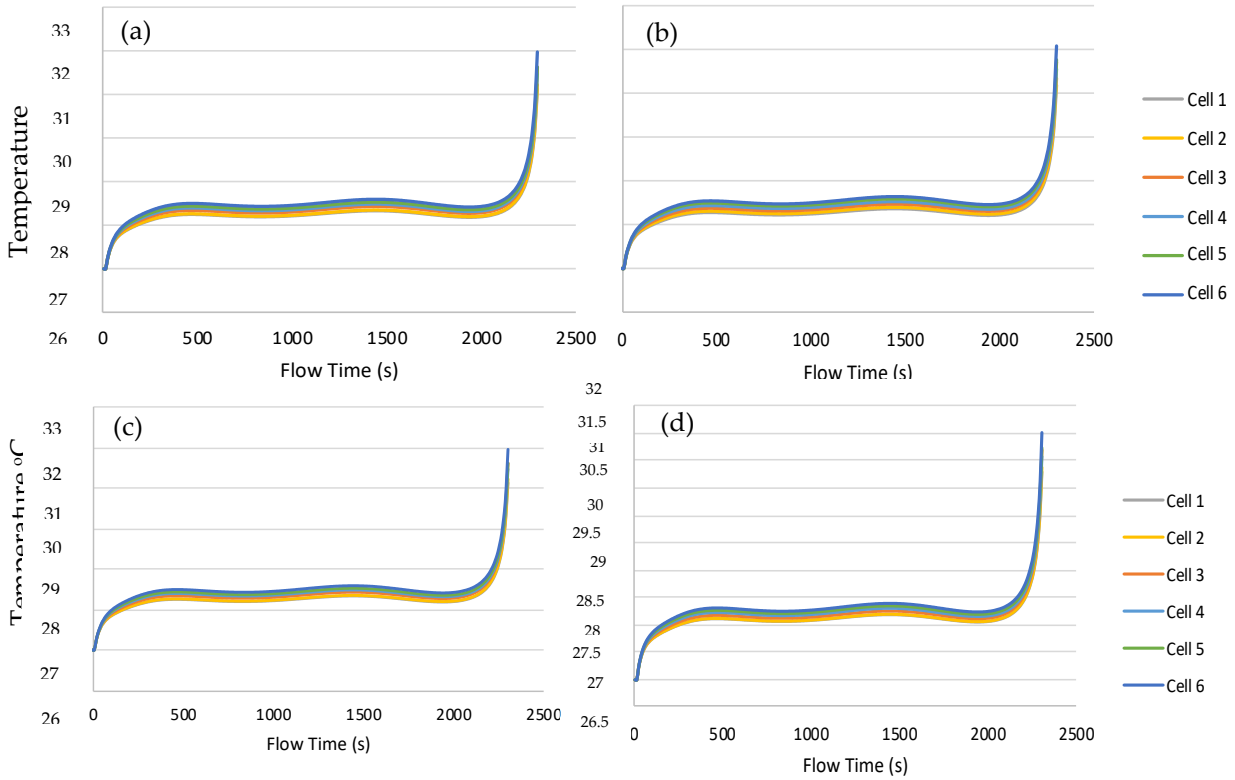

Figure 13. LIB cells temperature characteristic at 3C discharge rate with biodiesels cooling a) Jatropha, b) Karanj, c) Mahua, and d) Palm.

3.4.1. Parametric study of Palm cooling

In this section, Palm cooling has been analysed and optimised in terms of inlet velocity. If the inlet velocity is too high, the fuel pump would utilise excess energy, reducing the power efficiency of the system. If the velocity is too low, then the cooling efficiency will be affected due to the reduction in the Reynolds number.

Parametric analysis was performed to evaluate the impact of inlet velocity on the minimum and maximum temperatures and temperature differences across the LIB module of the Palm cooling. The relationship between maximum temperature and inlet velocity from the analysis is shown in Figure 14. There was a noticeable and linear change in the LIB module temperature for the inlet velocity of Palm cooling from 0.01 to 0.5 m/s. After 0.5m/s, the results converged and the increase in velocity did not significantly affect the LIB module temperature. This was due to the coolant flow being so turbulent, and the heat from the LIB module was removed very quickly as it almost matches the initial temperature of Palm. In terms of LIB maximum operating temperature, any velocity above 0.5 m/s would be over-designed as the change in temperature was minimal. However, it would mean that the LIB module would reduce in temperature quicker due to the increase in cooling efficiency.

Preprints (www.preprints.org) | NOT PEER-REVIEWED | Posted: 20 July 2022 doi:10.20944/preprints202207.0299.v1

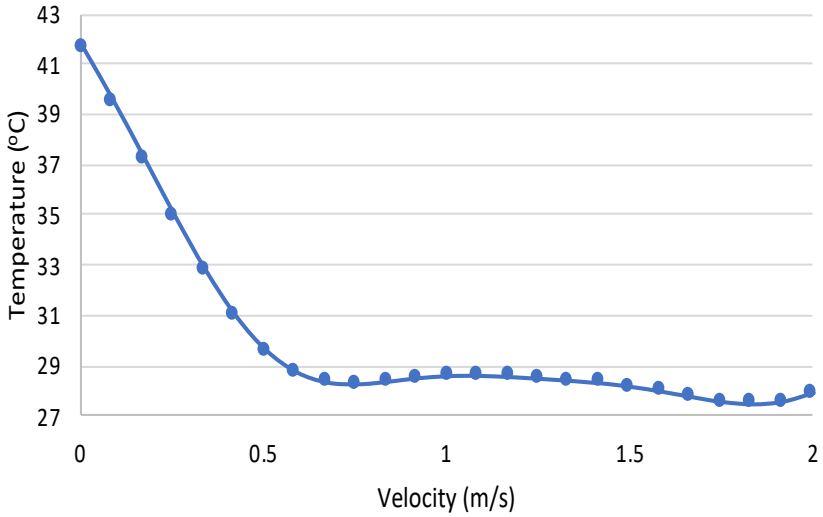

Figure 14. Relationship between LIB module maximum temperature and inlet velocity of Palm cooling at 3c discharge rate.

As shown in Figure 15, a similar trend was observed with the minimum temperature where after 0.5m/s, the increase in velocity did not affect the minimum temperature of the LIB module due to the high Reynolds number. Inlet velocities in the range of 0.25m/s to 0.5m/s were selected which ensures the LIB module was within the optimum working temperature. As a result of this large increase in velocities above the initial boundary condition of 0.09m/s, more energy is required to pump the coolant and a different fuel pump may be required for the increased velocities. The initial velocity was sufficient enough to keep the LIB module temperature within the optimum working temperature for the majority of the discharge time. However, depending on the application, the LIB module temperature may need to be further reduced or the coolant may need to be rapidly reduced, in which case a higher velocity can be used.

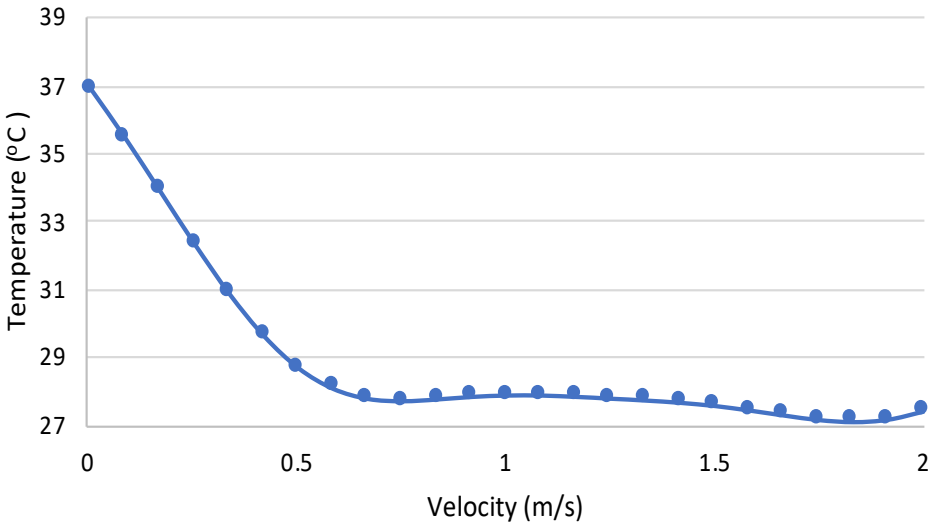

Figure 15. Relationship between LIB module minimum temperature and inlet velocity of Palm cooling at 3C discharge rate.

Figure 16 depicts the relationship between the temperature difference of LIB cells and inlet velocity. Also, a similar trend occurred when the result started to converge after 0.5m/s. However, the temperature difference of LIB cells was more sensitive in a bigger LIB module battery as a small difference in temperature can still have a large effect on the

Preprints (www.preprints.org) | NOT PEER-REVIEWED | Posted: 20 July 2022 doi:10.20944/preprints202207.0299.v1

LIB cell degradation. In this case, it might be best to use a higher inlet velocity to reduce significant temperature differences between LIB cells. On the other hand, the temperature difference between LIB cells can be negligible in some cases, so a lower inlet velocity can be adopted to reduce the pumping energy.

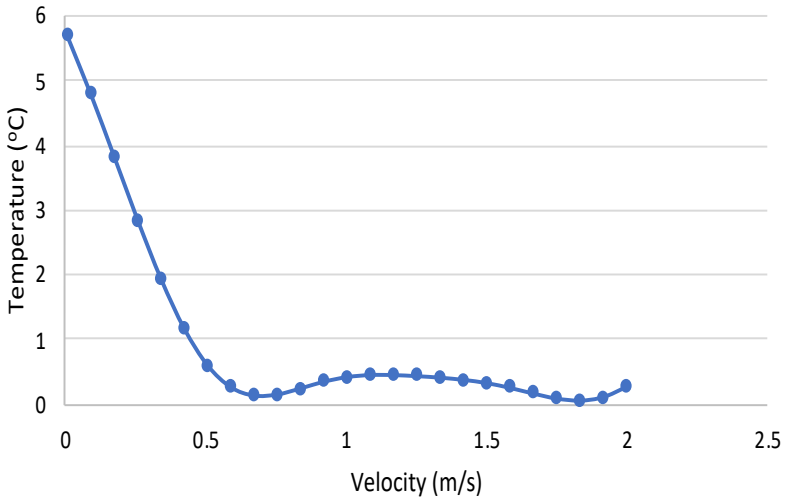

Figure 16. Relationship between LIB cell temperature difference and inlet velocity of Palm cooling at 3C discharge rate.

3.5. Comparative analysis of LIB module temperature

A comparison of air cooling, 3M Novec cooling, and biodiesel cooling showed the effectiveness of biodiesels in line with the current coolants used in industry. Figure 17 shows the LIB module temperature with each cooling medium along with benchmark data. The results showed that all cooling techniques used were effective in reducing the maximum temperature from benchmark results. However, air cooling did not sufficiently reduce the temperature of the LIB module, indicating that there is still an undesirable maximum temperature that would decrease the performance of the LIB module. This characteristic was caused by the low density of air, which reduced its Reynolds number.

3M Novec cooling provided the most effective solution with the lowest LIB module temperature control throughout the discharge cycle. Nevertheless, in comparison with biodiesel cooling, there was no significant difference in terms of cooling performance as both cooling strategies can maintain the LIB module temperature with the optimum operating temperature during the discharge cycle. The temperature characteristics of the LIB module with Palm, in addition to its low density compared to other biodiesels, make it the best candidate for BTMS. Also, it can be concluded that compared to 3M Novec cooling, Palm's cooling capacity is sufficient to compensate for the slight losses in cooling efficiency through the positive aspects of weight reduction.

Preprints (www.preprints.org) | NOT PEER-REVIEWED | Posted: 20 July 2022 doi:10.20944/preprints202207.0299.v1

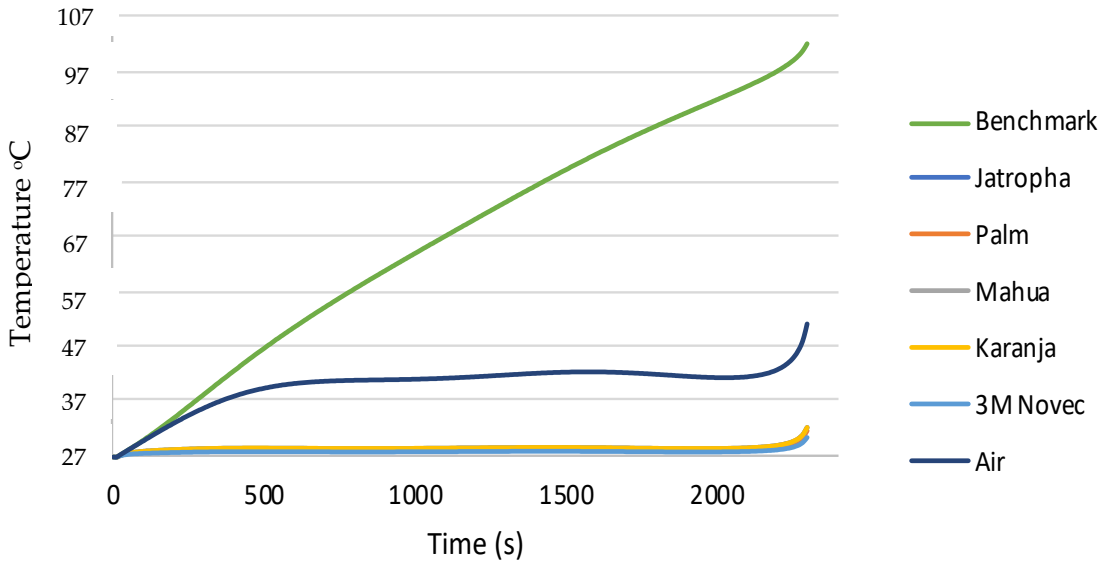

Figure 17. LIB module temperatures versus time using different cooling strategies at 3C discharge rate.

4. Conclusions

The LIB module was successfully analysed using a commercial CFD software Ansys Fluent to characterise the biodiesel in BTMS application. Four biodiesels were analysed, Palm, Jatropha, Mahua, and Karanja,and compared to more conventional coolants such as air and 3M Novec. These comparison studies allowed for the effectiveness of biodiesel cooling to be measured.A brief parametric study was established to determine the relationship between LIB temperature parameters and cooling inlet velocity. The key conclusions from the studies are the following:

- A benchmark LIB module without any means of cooling exceeded the maximum working temperature with the temperature increased linearly at different discharge rates. At a lower discharge rate of 0.5C, the LIB module maximum temperature exceeded the maximum working temperature by 5 °C when fully depleted. As the discharge rate increased to 3C, the LIB module maximum temperature reached 140 °C, which can cause thermal runaway. Also, the change in discharge rate affected the distribution of temperature across the LIB module. These results can significantly accelerate the LIB cells capacity degradation and performance, which in need of an efficient BTMS to control the LIB module within the optimum operating temperature range.
- Biodiesel cooling proved to be a very effective solution for BTMS with all the biodiesels being able to maintain the temperature within the optimum operating temperature range. The best biodiesel out of the four used was Palm as it managed to reduce the LIB module maximum temperature to 31.7 °C at discharge rate of 3, ensuring the LIB cells are working to its full potential and maintaining their lifespan. In addition, th low density of palm oil biodiesel (865kg/m^3) decreases the overall weight of the vehicle and the enclosure itself.
- Air cooling is a very inefficient method which could not maintain the LIB module temperature below the optimum range. In addition, the temperature gradient of the LIB module was 10 °C creating the issue of uneven cells voltage and leads to faster LIB cell degradation.. When compared with air cooling, biodiesel is a much better approach in terms of cooling efficiency and power efficiency from the fluid source as air requires higher velocities to improve cooling.

- 3M Novec performed the best out of the coolants in terms of maintaining the LIB optimum operating temperature. 3M Novec managed to maintain the LIB module temperature gradient at a desired temperature range. However, 3M Novec is heavy and thus increases the overall vehicle energy consumption, expensive and requires a complex system installation.Palm is a viable option to use as an alternative to 3M Novec. Although there is a slight reduction in cooling performance when compared with 3M fluid, Palm can maintain both LIB module optimum operating temperature and temperature gradients. The advantage to using Palm is the lower density which would reduce the weight of the enclosure by almost 43%. This weight reduction is a big advantage for performance applications and general HEV as it improves fuel economy.
- Finally, a parametric study was carried out to see the relationship between LIB module temperature parameters and cooling inlet velocity. The results demonstrated a convergence where after 0.5m/s, the parameters were not affected by the cooling inlet velocity and any increase would correlate with an increase in pumping power required.

References

1. *Renewable Energy - Resources, Challenges and Applications*; Al Qubeissi, M., El-kharouf, A., Serhad Soyhan, H., Eds.; IntechOpen, 2020; ISBN 978-1-78984-283-8.
2. Hansen, T.A. Stranded Assets and Reduced Profits: Analyzing the Economic Underpinnings of the Fossil Fuel Industry's Resistance to Climate Stabilization. *Renewable and Sustainable Energy Reviews* **2022**, *158*, 112144, doi:10.1016/j.rser.2022.112144.
3. Monasterolo, I.; Raberto, M. The Impact of Phasing out Fossil Fuel Subsidies on the Low-Carbon Transition. *Energy Policy* **2019**, *124*, 355–370, doi:10.1016/j.enpol.2018.08.051.
4. *Biofuels - Challenges and Opportunities*; Al Qubeissi, M., Ed.; IntechOpen, 2019; ISBN 978-1-78985-535-7.
5. Al Qubeissi, M. Predictions of Droplet Heating and Evaporation: An Application to Biodiesel, Diesel, Gasoline and Blended Fuels. *Applied Thermal Engineering* **2018**, *136*, 260–267, doi:10.1016/j.applthermaleng.2018.03.010.
6. Al Qubeissi, M.; Sazhin, S.S.; Elwardany, A.E. Modelling of Blended Diesel and Biodiesel Fuel Droplet Heating and Evaporation. *Fuel* **2017**, *187*, 349–355, doi:10.1016/j.fuel.2016.09.060.
7. Al-Esawi, N.; Al Qubeissi, M.; Kolodnytska, R. The Impact of Biodiesel Fuel on Ethanol/Diesel Blends. *Energies* **2019**, *12*, 1804, doi:10.3390/en12091804.
8. Kaliaperumal, M.; Dharanendrakumar, M.S.; Prasanna, S.; Abhishek, K.V.; Chidambaram, R.K.; Adams, S.; Zaghib, K.; Reddy, M.V. Cause and Mitigation of Lithium-Ion Battery Failure—A Review. *Materials* **2021**, *14*, 5676, doi:10.3390/ma14195676.
9. Allafi, W.; Uddin, K.; Zhang, C.; Mazuir Raja Ahsan Sha, R.; Marco, J. On-Line Scheme for Parameter Estimation of Nonlinear Lithium Ion Battery Equivalent Circuit Models Using the Simplified Refined Instrumental Variable Method for a Modified Wiener Continuous-Time Model. *Applied Energy* **2017**, *204*, 497–508, doi:10.1016/j.apenergy.2017.07.030.
10. Ma, S.; Jiang, M.; Tao, P.; Song, C.; Wu, J.; Wang, J.; Deng, T.; Shang, W. Temperature Effect and Thermal Impact in Lithium-Ion Batteries: A Review. *Progress in Natural Science: Materials International* **2018**, *28*, 653–666.
11. Chen, D.; Jiang, J.; Kim, G.-H.; Yang, C.; Pesaran, A. Comparison of Different Cooling Methods for Lithium Ion Battery Cells. *Applied Thermal Engineering* **2016**, *94*, 846–854.

12. Pesaran, A.; Santhanagopalan, S.; Kim, G.H. *Addressing the Impact of Temperature Extremes on Large Format Li-Ion Batteries for Vehicle Applications (Presentation)*; National Renewable Energy Lab. (NREL), Golden, CO (United States), 2013;
13. Roe, C.; Feng, X.; White, G.; Li, R.; Wang, H.; Rui, X.; Li, C.; Zhang, F.; Null, V.; Parkes, M.; et al. Immersion Cooling for Lithium-Ion Batteries – A Review. *Journal of Power Sources* **2022**, *525*, 231094, doi:10.1016/j.jpowsour.2022.231094.
14. Saw, L.H.; Tay, A.A.O.; Zhang, L.W. Thermal Management of Lithium-Ion Battery Pack with Liquid Cooling. In Proceedings of the 2015 31st thermal measurement, modeling & management symposium (SEMI-THERM); IEEE, 2015; pp. 298–302.
15. Kim, J.; Oh, J.; Lee, H. Review on Battery Thermal Management System for Electric Vehicles. *Applied thermal engineering* **2019**, *149*, 192–212.
16. Mohammed, A.G.; Elfeky, K.E.; Wang, Q. Recent Advancement and Enhanced Battery Performance Using Phase Change Materials Based Hybrid Battery Thermal Management for Electric Vehicles. *Renewable and Sustainable Energy Reviews* **2022**, *154*, 111759, doi:10.1016/j.rser.2021.111759.
17. Bibin, C.; Vijayaram, M.; Suriya, V.; Ganesh, R.S.; Soundarraj, S. A Review on Thermal Issues in Li-Ion Battery and Recent Advancements in Battery Thermal Management System. *Materials Today: Proceedings* **2020**, *33*, 116–128.
18. Wen, J.; Yu, Y.; Chen, C. A Review on Lithium-Ion Batteries Safety Issues: Existing Problems and Possible Solutions. *Materials express* **2012**, *2*, 197–212.
19. Troxler, Y.; Wu, B.; Marinescu, M.; Yufit, V.; Patel, Y.; Marquis, A.J.; Brandon, N.P.; Offer, G.J. The Effect of Thermal Gradients on the Performance of Lithium-Ion Batteries. *Journal of Power Sources* **2014**, *247*, 1018–1025.
20. Pesaran, A.A. Battery Thermal Management in EV and HEVs: Issues and Solutions. *Battery Man* **2001**, *43*, 34–49.
21. Raja Shah, R.M.; Jardine, B. THERMAL MANAGEMENT UNIT AND SYSTEM 2018. *Patent: US 11,001,123 B2*.
22. Wegmann, S.; Rytka, C.; Diaz-Rodenas, M.; Werlen, V.; Schneeberger, C.; Ermanni, P.; Caglar, B.; Gomez, C.; Michaud, V. A Life Cycle Analysis of Novel Lightweight Composite Processes: Reducing the Environmental Footprint of Automotive Structures. *Journal of Cleaner Production* **2022**, *330*, 129808, doi:10.1016/j.jclepro.2021.129808.
23. Wang, Y.; Biswas, A.; Rodriguez, R.; Keshavarz-Motamed, Z.; Emadi, A. Hybrid Electric Vehicle Specific Engines: State-of-the-Art Review. *Energy Reports* **2022**, *8*, 832–851, doi:10.1016/j.egyr.2021.11.265.
24. Al Qubeissi, M.; Almshahy, A.; Mahmoud, A.; Al-Asadi, M.T.; Shah, R.M.R.A. Modelling of Battery Thermal Management: A New Concept of Cooling Using Fuel. *Fuel* **2022**, *310*, 122403.
25. Cao, W.; Zhao, C.; Wang, Y.; Dong, T.; Jiang, F. Thermal Modeling of Full-Size-Scale Cylindrical Battery Pack Cooled by Channeled Liquid Flow. *International Journal of Heat and Mass Transfer* **2019**, *138*, 1178–1187, doi:10.1016/j.ijheatmasstransfer.2019.04.137.
26. Eastop, T.D.; McConkey, A. *Applied Thermodynamics for Engineering Technologists*; Pearson/Prentice Hall, 2006;
27. Tu, J.; Yeoh, G.-H.; Liu, C. CFD Mesh Generation: A Practical Guideline. In *Computational Fluid Dynamics*; Elsevier, 2018; pp. 125–154 ISBN 978-0-08-101127-0.
28. Al Qubeissi, M.; Sazhin, S.S.; Crua, C.; Turner, J.; Heikal, M.R. Modelling of Biodiesel Fuel Droplet Heating and Evaporation: Effects of Fuel Composition. *Fuel* **2015**, *154*, 308–318, doi:10.1016/j.fuel.2015.03.051.
29. Sazhin, S.S.; Al Qubeissi, M.; Kolodnytska, R.; Elwardany, A.E.; Nasiri, R.; Heikal, M.R. Modelling of Biodiesel Fuel Droplet Heating and Evaporation. *Fuel* **2014**, *115*, 559–572, doi:10.1016/j.fuel.2013.07.031.

30. Yasin, M.H.M.; Mamat, R.; Sharma, K.; Yusop, A.F. Influence of Palm Methyl Ester (PME) as an Alternative Fuel in Multicylinder Diesel Engine. *Journal Mechanical Engineering and Sciences* **2012**, *3*, 331–339.

31. Takase, M.; Zhao, T.; Zhang, M.; Chen, Y.; Liu, H.; Yang, L.; Wu, X. An Expatiate Review of Neem, Jatropha, Rubber and Karanja as Multipurpose Non-Edible Biodiesel Resources and Comparison of Their Fuel, Engine and Emission Properties. *Renewable and Sustainable Energy Reviews* **2015**, *43*, 495–520.

32. Manjunath, M.; Prakash, P.; Raghavan, V.; Mehta, P.S. Composition Effects on Thermo-Physical Properties and Evaporation of Suspended Droplets of Biodiesel Fuels. *SAE International Journal of Fuels and Lubricants* **2014**, *7*, 833–841.

33. Huber, C.; Kuhn, R. Thermal Management of Batteries for Electric Vehicles. In *Advances in battery technologies for electric vehicles*; Elsevier, 2015; pp. 327–358.

34. Teng, H. Thermal Analysis of a High-Power Lithium-Ion Battery System with Indirect Air Cooling. *SAE International Journal of Alternative Powertrains* **2012**, *1*, 79–88.

35. 3M™ Novec™ 7000 Engineered Fluid Available online: https://www.3m.com/3M/en_US/company-us/SDS-search/ (accessed on 28 July 2021).